32nd URSI GASS, Montreal, 19–26 August 2017

Spatial and temporal ionospheric monitoring using broadband sferic measurements

Jackson C. McCormick*(1), Morris B. Cohen(1)
(1) Georgia Institute of Technology, Atlanta, GA, 30319

Abstract

The D-region of the ionosphere (60-90 km altitude) is highly variable on timescales from fractions of a second to many hours, and on spatial scales from 10 km to many hundreds of km. VLF and LF (3-30kHz, 30-300kHz) radio waves are guided to global distances by reflecting off of the ground and the D-region. Therefore, information about the current state of the ionosphere is encoded in received VLF/LF radio waves since they act like probes of the D-region. The return stroke of lightning is an impulsive event that radiates powerful broadband radio emissions in the VLF/LF bands. Lightning is spread broadly in space and time allowing for much greater spatial and temporal study of the D-region when compared to past VLF transmitter-based studies. Furthermore, the broadband nature of lightning allows more spectral information compared to a single frequency VLF wave generated by VLF transmitters. Individual lightning-generated waveforms, or 'sferics', can vary due to varying lightning current parameters, D-region ionospheric variabilities, or location/timing uncertainty. We describe a technique to recover the amplitude and phase of sferics and quantify the detectability of an ionospheric change, such as from solar flares and other natural ionospheric disturbances, from their spectra change. We demonstrate the utility of our technique with ambient and varied ionospheric conditions. This technique allows for simultaneous study of spatial and temporal ionospheric variation and detection of ionospheric disturbances.

1 Introduction

The D-region of the ionosphere ($\sim$60$-$90 km) is a relatively inaccessible but important region for subionospheric radio propagation. The D-region varies spatially and temporally due to solar effects over diurnal, seasonal, and solar cycle based periods. Unfortunately, the D-region is very difficult to characterize as it is too high for balloons, too low for satellites, and not sufficiently ionized for radars. Rocket-based measurements produce good ionospheric profile results, but they cannot realistically be applied on a continuous and global basis.

Terrestrial Very Low Frequency (VLF, 3$-$30 kHz) and Low Frequency (LF, 30$-$300 kHz) waves propagate to global distances guided by the earth ground and the D-region of the ionosphere commonly known as the Earth-ionosphere waveguide (EIWG). Therefore, propagating VLF/LF signals carry with them information about the current state of the D-region. Because of this global propagation and since waves are able to penetrate significantly into water via the skin effect, various navies have constructed and operated VLF transmitters for the purposes of submarine communications. These transmitters operate almost continuously at constant power and frequency allowing an observer to serendipitously use them to monitor the current conditions of the ionosphere. Thomson (1993) used these VLF transmitters along with the Wait parameters H' and β (Wait and Spies, 1964) (Or effective reflection height and exponential steepness of an assumed exponentially-linear profile) and the Long Wave Propagation Capability (LWPC) code, to measure and monitor H' and β. The LWPC code was developed to model VLF transmitter propagation throughout the Earth-ionosphere waveguide and has seen many improvements and updates, the latest version is described in (Ferguson, 1998).

Lightning flashes occur about 40$-$50 times per second throughout the Earth. An average of $\sim$2000 lightning storms occur each day with an mean duration of $\sim$30 minutes creating a broad spatial and temporal distribution of lightning-generated VLF/LF sources. The return stroke of a lightning flash generates powerful impulsive broadband radio wave packets in the VLF/LF bands known as 'radio atmospherics' or 'sferics'. These sferics also propagate efficiently (few dB per Mm) to global distances guided by the EIWG. Sferics therefore allow a convenient signal of opportunity to monitor ionospheric conditions along the path from the lightning source to a VLF/LF receiver. Using this hypothesis, Cummer et al. (1998) developed a technique of monitoring the modal interference pattern in sferic amplitude spectra to monitor the ionospheric electron density parameters H', β. Using time-domain sferics, Lay and Shao (2011) developed a technique to sense a small portion of the D-region corresponding to the Fresnel refraction zone or the region of the first ionospheric hop, and observed ionospheric disturbances in the effective reflection height and reflection loss. Using these same parameters and a full-wave model, Lay et al. (2014) inferred H' and β in the Fresnel refraction zone allowing for a small spatially averaged measurement. Both sferic-based techniques utilize key features of sferics that are specific to certain source-receiver distances or geometries, and are not generally applicable and neither technique utilizes phase spectra. In this paper

we describe a general technique to recover stable sferics for any source-receiver geometry including time-domain, amplitude, and phase spectra.

2 Data Description

We utilize VLF/LF (∼1-50 kHz) magnetic field data sampled by an instrument similar to the AWESOME receiver (Cohen et al., 2010). Two wire loops are mounted in the North/South and East/West directions to capture both horizontal magnetic field components. The magnetic field in the z or upward direction is very near to zero due to the boundary conditions established by earth ground being a good conductor at VLF/LF frequencies. The raw magnetic field data signal is first amplified, and then low-pass filtered to prevent aliasing. The signal is then sampled continuously at 1 MHz with 16-bit resolution and sensitivity of 0.1 fT/rt-Hz or better. The collected data is then time-synchronized to GPS reference for an absolute time value. All of the time-series data used in this work is from a receiver at Pisgah Astronomical Research Institute (PARI) near Rosman, NC, USA (N35.1996, W82.8718).

We utilize lightning location data from the GLD360 network operated by Vaisala inc. GLD360 utilizes a combination of time of arrival, sferic shape, and a network of AWESOME VLF receivers to geolocate lightning. The basic operating principles of this network are described in Said et al. (2010). GLD360 detects lightning with a global detection efficiency of greater than 70% and reports peak current estimates, polarity, location, and time of occurrence for each lightning event. The sferic waveform changes as a function of return stroke current parameters, distance, and propagation conditions such as path conductivity/permitivity or ionospheric state. The uncertainty and non-uniformity of propagation conditions lead to errors in lightning location estimates. Figure 2 shows the inherent sferic timing and location error-induced jitter in the left-hand panel, assuming the network's estimate is taken as absolute truth. In this example, the standard deviation of timing jitter is 15.02 μs.

For consideration of sferic propagation during solar flares we utilize data from the NOAA GOES 15 satellite which continuously monitors solar emissions including x-ray emissions in the XL(0.1-0.8 nm) XS(0.05-0.4 nm) regimes.

3 Methods

Our goal is to process sferics in such a way as to mitigate the effects of sferic jitter as discussed earlier. The block diagram depicting our solution is given in Figure 1.

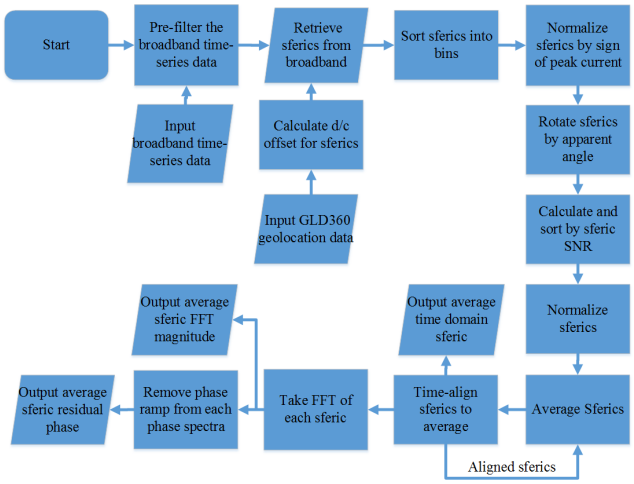

Figure 1. Block diagram of broadband sferic processing steps. Squares represent an individual processing step, while parallelograms represent inputs and outputs.

The two dominant sources of energy in the VLF/LF frequency band are lightning generated sferics and communications transmitters (Chrissan and Fraser-Smith, 1996). These VLF/LF beacons are used, for instance, by the US Navy at high power, with a very narrow bandwidth, for submarine communications. Therefore the entire time-series data is filtered using a zero phase notch filter to remove these transmitters.

We utilize the GLD360 location and timing estimate, and by assuming speed of light propagation delay, the propagation time from source to receiver is calculated and added to the reported time of the lightning stroke (We refer to this time as the d/c). Each sferic has a N/S component and an E/W component of magnetic field because of the geometry of the receiver antennas. We digitally rotate the two channels to maximize the energy on one channel between the period of 100 μs before d/c and 900 μs after d/c. We focus on the higher SNR channel for the remainder of this work.

Because propagation conditions are very similar for a limited time and location range, lightning occurring in similar locations and times are 'binned' together so that we can apply a superposed epoch analysis to arrive at an average or 'representative' sferic for that path and time. We ignore bins that have a count of less than 10 sferics. This averaging normalizes variations in received sferics due to lightning source parameter variability. The binned sferics are multiplied by their polarity (+ or -) so that positive an negative sferics are comparable. A representative sferic made up of all the sferics within a bin can be distorted by low-SNR sferics and by the timing jitter of received sferics as depicted in Figure 2. To automatically deselect outliers, the SNR of each sferic is directly measured. The SNR is calculated as follows: the signal value is measured by taking the moving average of the sferic magnitude with a window size of 40 μs. The peak value of this average is taken to be the signal value. To calculate the noise level, we find the RMS

value of the concatenated signal portion 200 μs before and 300 μs after the sferic. Sferics with an SNR of less than 5 (or 7dB) are removed for all of the examples in this paper.

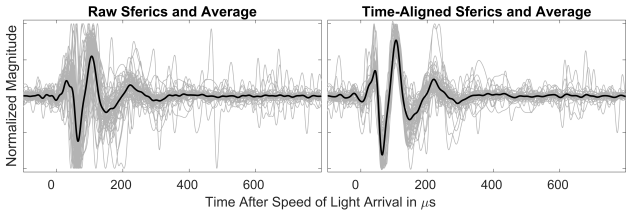

Figure 2. Example of time-aligning a bin and it's time-sferic average results. In both panels, all sferics in the bin are plotted in light gray. The left panel is the lightning reported results correcting for an assumed speed of light propagation. The right panel is the same sferics adjusted in time to line up. The black sferics in both plots are the average of the sferics in the respective panel.

In order to ensure that each sferic has the same weight in the processed representative sferic, each is normalized by its peak value. Even with low-SNR sferics removed, a time-based superposed epoch analysis gives mediocre results for a representative sferic because of the location and timing error induced jitter. This is easily seen in the left-hand panel of Figure 2 with each sferic in the bin plotted in grey. In order to remove the timing jitter, we must align all the sferics in each bin. We do this recursively: a raw average is taken of all of the sferics within a bin with no adjustment to the sferic jitter. Then each sferic within that bin is aligned to the raw average by finding the maximum cross correlation of the original sferic and the flipped sferic, allowing both polarities. A new average is taken with the aligned and/or flipped sferics. We continue this process iteratively until convergence occurs. After convergence, the final time-domain output is the average of the aligned sferics.

Past studies have utilized the spectral interference pattern for ionospheric sensing e.g. (Cummer et al., 1998). These studies used modal-interference patterns observed in sferic spectra, which is primarily a propagation effect making their techniques independent of lightning source parameters. Another advantage of frequency domain analysis is that the amplitude spectra is insensitive to timing jitter. We produce an averaged representative amplitude spectra sferic by taking the FFT of each sferic within a bin, and then taking the mean of magnitude of the FFT coefficients.

However, in order to recover stable phase spectra an additional step is necessary. The FFT's zero time reference is the beginning of the input signal. Since the VLF/LF group velocity is slower than the speed of light reference chosen in this work, there is a time-delay built into the signal. This time delay is the same as multiplying the Fourier transform by a complex exponential. The complex exponential adds a line to phase with the slope proportional to the time delay that we refer to as phase ramping. Any small timing jitter still present in the time-domain sferics will also manifest itself as an additional phase ramping. Because of the sensitivity of phase spectra to very small timing errors we calculate and output a residual phase by removing all phase ramping.

Phase ramping on orders greater than 360 degrees will usually be 'wrapped' between 0 and 360 degrees due to phase ambiguity above 360 degrees. Therefore each signal is unwrapped with a 180 degree reference resulting in the raw phase that appears as linear with some details. A linear trend is fit between between 9 and 30 kHz, the portion of the signal we empirically determined to be the highest-SNR portion of the signal. This linear fit is removed from the unwrapped phase of the signal and what remains is the details or residual phase. The final residual phase spectrum is the average of the residual phase of each sferic within a bin. Importantly, this result is now insensitive to small timing jitter.

4 Results

In order to quantify the effectiveness of this technique, we measure sferic variability for several examples. During the period 2015/09/01-2015/09/15 there was very little x-ray solar activity. This implies that daytime ionospheric variability was relatively minimal. For the region over Panama, 12 of the 15 days had lightning from 19:37:30−19:52:30 UT. For the 12 lightning days, their binned and processed amplitude and phase are plotted in Figure 3 in grey. The mean of the waveforms is plotted in black and some sample error bars are shown

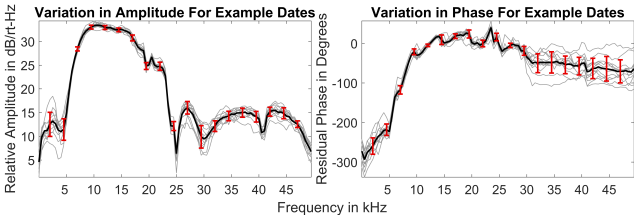

Figure 3. Illustration of calculated error bars. In the both panels, all available representative sferics from 2015/09/01−2015/09/15 are plotted in light gray. The mean is plotted in black, while the linear standard deviation is represented each direction from the mean in red plotted at 2.5 kHz intervals. The left box includes amplitude waveforms while the right-hand panel shows the calculated residual phase waveforms.

The error bar calculation demonstrates the expected variation for the example geometry. But in principle, such error bars can be calculated for any path. When comparing sferics for a similar geometry, exceeding these error bars indicates that the ionospheric conditions are different than the expected ambient conditions. Different ionospheric disturbances may affect sferic spectra differently, so the pattern of spectra changes may indicate the type of event. Figure 4 shows the error bars applied to a test day of 2015/08/21. The left panels show amplitude and phase for quiet solar

conditions near local noon. Since the sferics fall within the error bars, these sferics indicate stable or normal ionospheric conditions. In the right-hand panels, sferics are shown for known different ionospheric conditions.

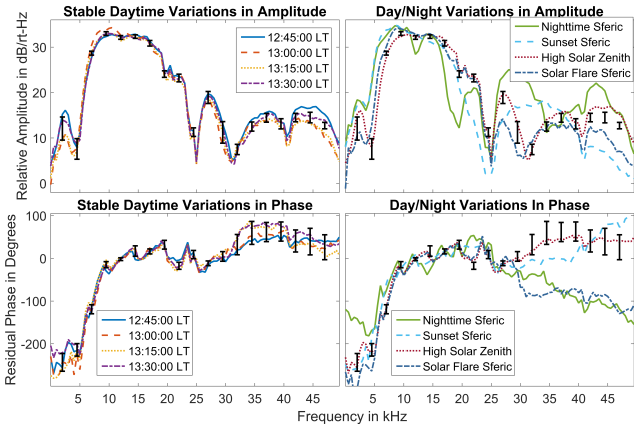

Figure 4. Example of processing stability and demonstration of detectability of variations in ionospheric structure. The top two figures are amplitude, while the bottom two are phase. The left two panels are stable ionospheric conditions (Near local high-noon, with normal solar activity). The right two panels are examples from solar conditions that cause known ionospheric variability.

These sferics drastically violate the error bars indicating a modified ionosphere versus the stable daytime ionosphere. This allows for ionospheric monitoring with a known confidence. With high-quality sferics in both time and amplitude/phase domains, a generalized approach to ionospheric characterization of any source/receiver geometry may be possible. The various studies have shown different inferred H' and β based on different sferic domain waveforms, but including sferic phase in these techniques or a new technique may help resolve these discrepancies.

5 Summary

Lightning is a powerful impulsive and broadband source of VLF/LF radiation which is sensitive to the current state of the D-region ionosphere due to its reflection from the region. These lightning-generated signals or sferics are spread broadly in space and time allowing for greater spatial coverage of the ionosphere when compared to VLF single-frequency transmitters.

Even the best lightning location networks have small errors in location and time of occurrence which create difficulties in recovering an accurate time-based solution or spectral phase. We described a technique to recover time-based, amplitude spectra, and phase spectra simultaneously, while also mitigating variability of lightning return stroke sources.We demonstrated the utility of this technique by comparing measured data to cases of known ionospheric stability and variability.

Sferics have been utilized to remotely sense the D-region by using both amplitude spectra and time-based techniques for a small number of geometries. But these techniques are dependent on certain geometries and have not utilized the full availability of data. Future work will focus on producing ionospheric inferences which will be informed by the full breadth of information recovered by this technique.

6 Acknowledgements

This research was supported by NSF grant AGS 1451142. We are very grateful to the Pisgah Astronomical Research Institute and to its staff for their continued support and collaboration.

References

N. R. Thomson, "Experimental daytime vlf ionospheric parameters," *Journal of Atmospheric and Terrestrial Physics*, vol. 55, no. 2, pp. 173–184, June 1993.

J. R. Wait and K. P. Spies, "Characteristics of the earth-ionosphere waveguide for vlf radio waves," National Bureau of Standards, Technichal Note 300, 1964.

J. A. Ferguson, "Computer programs for assessment of long-wavelength radio communications," Space and Naval Warfare Systems Center, San Diego, Tech. Rep. 3030, 1998.

S. A. Cummer, U. S. Inan, and T. F. Bell, "Ionospheric d region remote sensing using vlf radio atmospherics," *Radio Science*, vol. 33, no. 6, pp. 1781–1792, 1998.

E. H. Lay and X.-M. Shao, "Multi-station probing of thunderstorm-generated d-layer fluctuations by using time-domain lightning waveforms," *Geophys. Res. Lett.*, vol. 38, no. 23, pp. n/a–n/a, 2011. [Online]. Available: http://dx.doi.org/10.1029/2011GL049790

E. H. Lay, X.-M. Shao, and A. R. Jacobson, "D region electron profiles observed with substantial spatial and temporal change near thunderstorms," *J. Geophys. Res. Space Physics*, vol. 119, no. 6, pp. 4916–4928, 2014. [Online]. Available: http://dx.doi.org/10.1002/2013JA019430

M. B. Cohen, U. S. Inan, and E. W. Paschal, "Sensitive broadband elf/vlf radio reception with the awesome instrument," *IEEE Transactions on Geoscience and Remote Sensing*, vol. 48, no. 1, January 2010.

R. K. Said, U. S. Inan, and K. L. Cummins, "Long-range lightning geolocation using a vlf radio atmospheric waveform bank," *Journal of Geophysical Research*, vol. 115, no. D23, December 2010.

D. A. Chrissan and A. C. Fraser-Smith, "Seasonal variations of globally measured elf/vlf radio noise," *Radio Sci.*, vol. 31, no. 5, pp. 1141–1152, 1996. [Online]. Available: http://dx.doi.org/10.1029/96RS01930